APL Materials

High output power density and strong vibration durability in a modified barbell-shaped energy harvester based on multilayer $Pb(In_{1/2}Nb_{1/2})O_3$–$Pb(Mg_{1/3}Nb_{2/3})O_3$–$PbTiO_3$ single crystals

Cite as: APL Mater. **9**, 010703 (2021); https://doi.org/10.1063/5.0035474
Submitted: 28 October 2020 • Accepted: 27 December 2020 • Published Online: 25 January 2021

Jinfeng Liu, Xiangyu Gao, Chaorui Qiu, et al.

AIP Publishing

High output power density and strong vibration durability in a modified barbell-shaped energy harvester based on multilayer $Pb(In_{1/2}Nb_{1/2})O_3$–$Pb(Mg_{1/3}Nb_{2/3})O_3$–$PbTiO_3$ single crystals

Cite as: APL Mater. 9, 010703 (2021); doi: 10.1063/5.0035474
Submitted: 28 October 2020 • Accepted: 27 December 2020 •
Published Online: 25 January 2021

Jinfeng Liu, Xiangyu Gao,[a] Chaorui Qiu, Liao Qiao, Jingya Yang, Ming Ma, Kexin Song, Haisheng Guo, Zhuo Xu, and Fei Li[a]

AFFILIATIONS

Electronic Materials Research Laboratory (Key Laboratory of Education Ministry), State Key Laboratory for Mechanical Behavior of Materials and School of Electronic Science and Engineering, Xi'an Jiaotong University, Xi'an, China

Note: This paper is part of the Special Topic on 100 Years of Ferroelectricity—A Celebration.

[a]**Authors to whom correspondence should be addressed:** gaoxiangyu@xjtu.edu.cn and ful5@xjtu.edu.cn

ABSTRACT

Traditional piezoelectric energy harvesters are made of piezoelectric ceramics with a cantilever structure, which show a low output energy density. Thus, they are difficult to meet the requirements for self-powered electronics. Herein, we report a modified barbell-shaped piezoelectric energy harvester (BSPEH) based on two d_{33}-mode cuboid $Pb(In_{1/2}Nb_{1/2})O_3$–$Pb(Mg_{1/3}Nb_{2/3})O_3$–$PbTiO_3$ multilayer single crystal stacks (ten wafers with a thickness of 0.5 mm and $d_{33} \sim 1300$ pC/N). Due to the electrically parallel and series connections of multilayer piezoelectric elements and the high figure-of-merit $d_{33} \times g_{33}$ of the single crystal, the maximum power density of BSPEH could reach 39.7 mW cm^{-3} (under an acceleration of 5 g), which is much higher than that of traditional cantilever piezoelectric energy harvesters (CPEHs), ~0.1 mW cm^{-3}. A maximum output voltage of 50.4 V_{p-p} was obtained when two crystal stacks are connected in series, and a maximum output current of 880 μA can be obtained when two crystal stacks are connected in parallel. Furthermore, the energy harvesting properties of BSPEH stay almost the same after 10^6 vibration cycles, while the properties of CPEH decrease 20% after 10^5 vibration cycles. This work indicates that BSPEH has a great potential in the application of wireless sensor networks for realizing the self-power of the equipment.

I. INTRODUCTION

Recently, due to the potential applications in wireless sensing technology, portable electronic devices, and the Internet of Things (IoT), the collection of thermal, light, mechanical vibration, and other energy sources in the natural environment has become a research hotspot.[1–3] Among these renewable energy sources, mechanical vibration energy is not limited by the region, time, and weather and can be found everywhere in human activity, machine running, pipelines, bridges, and so on. In particular, using the piezoelectric energy harvesters for vibration energy harvesting has attracted great attention due to their simple structure, high energy density, and miniaturization,[4,5] compared to electrostatic[6,7] or electromagnetic mechanisms.[8] However, the output energy densities of piezoelectric energy harvesters are still not high enough to meet the requirements of practical applications. Thus, it is highly required to optimize the configuration to improve the power density and energy conversion efficiency. In addition, for the traditional cantilever structure, the piezoelectric element is easy to break under the large acceleration, load, or long time running.[9]

To improve the output performance of the energy harvester, considerable efforts and new designs have been made. Ma *et al.*[10] used the piezoelectric unimorph energy harvester with perpendicular electrodes to obtain shear and transverse piezoelectric effects, producing 1.5 times open-circuit voltage and 3.9 times power, compared with the traditional electrode. Ren *et al.*[11] designed a cymbal transducer for energy harvesting, which can withstand a larger force. However, these conventional unimorph structure designs did not avoid the cracking of piezoelectric elements during the long time working. Then, Li *et al.*[9] reported a flex-compressive (F–C) mode energy harvester that works under pressure conditions, improving the working life of the energy harvester. However, it has a low output power density. Yuan *et al.*[4] used 3D-printed multilayer poly(vinylidene fluoride-co-trifluoroethylene) (PVDF-TrFE) copolymers to fabricate a rugby ball energy harvester and obtained high output performance and cycling stability. However, its high matching impedance results in an inferior energy transmission efficiency. In 2016, Wu *et al.*[12] proposed a barbell-shaped energy harvester, which can effectively improve the cracking problem of the traditional cantilever structure. On this basis, Gao *et al.*[13] successfully increased the output voltage and power by using piezoelectric disks with separated surface electrodes. In addition to modification of the structure, the power density of the energy harvesters can be enhanced with respect to piezoelectric materials. Compared with the state-of-the-art Pb(Zr, Ti)O_3 (PZT) ceramics and lead-free ceramics, relaxor-$PbTiO_3$ (PT) based ferroelectric single crystals possess much higher electromechanical coupling factors, piezoelectric coefficient, and figure-of-merit (FOM).[14,15] Thus, using relaxor ferroelectric crystals, such as $Pb(Mg_{1/3}Nb_{2/3})O_3$–$PbTiO_3$ (PMN-PT) and $Pb(In_{1/2}Nb_{1/2})O_3$–$Pb(Mg_{1/3}Nb_{2/3})O_3$–$PbTiO_3$ (PIN-PMN-PT), is expected to obtain a higher energy density. For example, Zeng *et al.*[16] reported an energy harvester composed of two symmetrically assembled sandwich-type PMN-PT single crystals and a cantilever. However, the two sandwich-type single crystals of the device cannot contribute to the output performance simultaneously. Gao *et al.*[5] designed a shear-mode piezoelectric energy harvester based on the PIN-PMN-PT crystal, which obtained three times power density compared with the same structure harvester based on piezoelectric ceramics. However, its resonant frequency (f_r) is up to 1 kHz, so it is difficult to find a suitable vibration ambient.

In this paper, the energy harvester has been modified from two aspects to obtain a high energy density and good structural stability. First, we used the high-performance relaxor ferroelectric single crystals (PIN-PMN-PT) as the core piezoelectric elements to improve the output performance of the device. Second, a modified barbell-shaped structure was employed to assemble the energy harvester. Here, we designed a barbell-shaped piezoelectric energy harvester (BSPEH) based on two cuboid PIN-PMN-PT crystal stacks. These stacks with a large piezoelectric coefficient operate in the d_{33}-mode. Because the piezoelectric material is in a clamping state and works under pressure conditions, the structure can stand up to a large vibration amplitude excitation and has strong vibration durability. Then, the structure was optimized by the finite element method (FEM). The output current, voltage, and power of the BSPEH were tested. Finally, the durability of the cantilever piezoelectric energy harvester (CPEH) and BSPEH was measured when the output voltage and the inertial force were almost the same, which proves that the BSPEH has great potential applications under large vibration amplitude excitation and long time working.

II. DESIGN OF THE BSPEH

As shown in Fig. 1, the BSPEH consists of two single crystal stacks [4.4 mm (L) × 4.4 mm (W) × 5.6 mm (H)] and a spring steel fixture. The single crystal wafers are poled along the thickness direction, as shown in Fig. 1(b). Each crystal stack is fabricated of ten crystal wafers stacking in opposite polarity and connected by epoxy. The two stacks are fixed on the base by a steel cover and flange shaft. A 5.0 g ring-type copper plate is installed at the other end of the flange shaft as a tip mass to generate the acceleration force under mechanical vibration excitation. L_1 is the length of the flange shaft

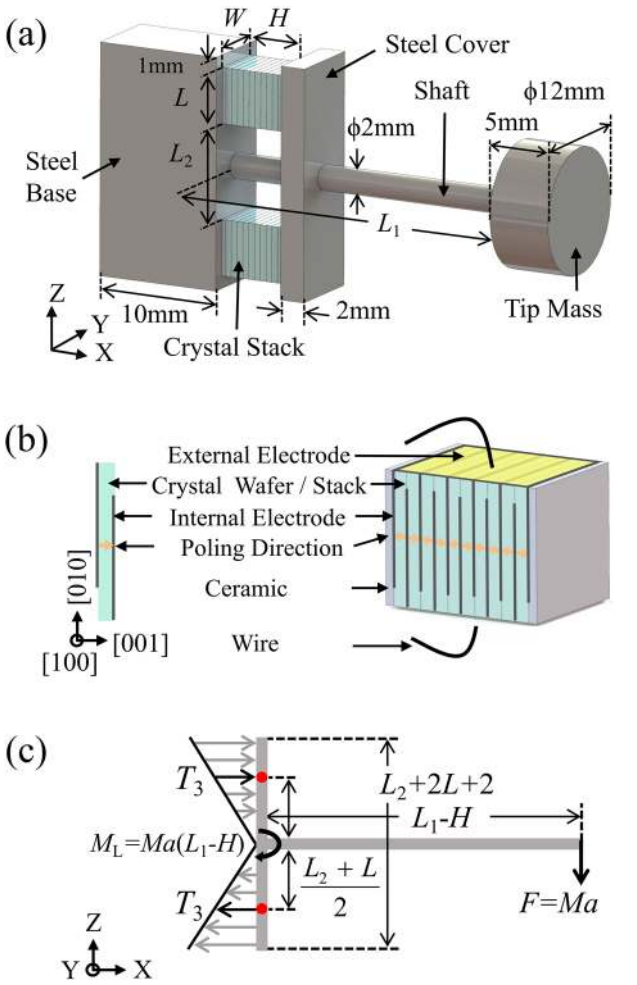

FIG. 1. Schematic of the proposed barbell-shaped piezoelectric energy harvester (BSPEH). (a) The structure of the BSPEH. (b) The enlarged view of the crystal stack in (a). (c) Mechanical analysis of the structure. The gray arrows represent the normal stress distribution on the cross section, and the red dots represent the top surface center of the crystal stacks.

and L_2 is the distance between two crystal stacks, shown in Fig. 1(a). The output characteristics are measured under two conditions: (1) two stacks connected in series and (2) two stacks connected in parallel.

A. Mechanical analysis

As the vibration acceleration a is applied, the tip mass M can produce an inertial force of Ma, as shown in Fig. 1(c). This inertial force further produces a bending moment of $M_L = Ma(L_1 - H)$ (where $H = 5.6$ mm is the height of the single crystal stack), which dynamically applies an equivalent axial stress T_3 to the piezoelectric stacks via the connected flange shaft, causing the stacks to operate in the d_{33}-mode. According to the cantilever beam model, T_3 can be approximately estimated as

$$T_3 = \frac{Ma(L_1 - H)(L_2 + L)}{2I_z}, \tag{1}$$

where $L = 4.4$ mm is the length of the single crystal stack and $I_z = \frac{(W+2)(L_2+2L+2)^3}{12}$ is the moment of inertia of the steel cover section (where $W = 4.4$ mm is the width of the single crystal stack). The axial force F_N caused by vibration acceleration a is

$$F_N = T_3 LW = \frac{6Ma(L_1 - H)(L_2 + L)LW}{(W + 2)(L_2 + 2L + 2)^3}. \tag{2}$$

According to the piezoelectric equation, the induced electric displacement D_{33} can be expressed as

$$D_{33} = d_{33}T_3 = \frac{6d_{33}Ma(L_1 - H)(L_2 + L)}{(W + 2)(L_2 + 2L + 2)^3}, \tag{3}$$

where d_{33} is the longitudinal piezoelectric coefficient of the crystal wafer. Under the excitation of vibration acceleration, the induced charge Q, corresponding output short-circuit current peak I_p, and open-circuit voltage peak V_p from one stack can be expressed as[4]

$$Q = D_{33}LWn = \frac{6nd_{33}Ma(L_1 - H)LW(L_2 + L)}{(W + 2)(L_2 + 2L + 2)^3}, \tag{4}$$

$$I_p = j(2\pi)fQ = \frac{12j\pi fnd_{33}Ma(L_1 - H)LW(L_2 + L)}{(W + 2)(L_2 + 2L + 2)^3}, \tag{5}$$

$$V_p = \frac{Q}{nC_0} = \frac{6g_{33}Ma(L_1 - H)(L_2 + L)t}{\varepsilon_0(W + 2)(L_2 + 2L + 2)^3}, \tag{6}$$

where n is the layers of the crystal stack, C_0 is the static capacitance of one piece of crystal wafer, f is the vibrational frequency, $g_{33} = \frac{d_{33}}{\varepsilon_{33}^T}$ is the longitudinal piezoelectric coefficient of the crystal wafer, t is the thickness of the crystal wafer, and ε_0 is the vacuum dielectric permittivity.

Since the single crystal stack is in the state of mechanical series and electrical parallel, for one single crystal stack, the mechanical-vibration-induced charge Q increases by n (the number of crystal wafers in a crystal stack) times, but the voltage will remain the same because the capacitance C_0 will also increase by n times [as shown in Eqs. (4) and (6)]. According to Eq. (6), it can be inferred that the output voltage of the BSPEH is proportional to d_{33}, the vibration acceleration a, and the size of the BSPEH. The peak output power P_p from one stack can be calculated as follows:

$$P_p = \frac{V_p I_p}{2} = \frac{36j\pi fnd_{33}g_{33}M^2a^2(L_1 - H)^2LW(L_2 + L)^2t}{\varepsilon_0(W + 2)^2(L_2 + 2L + 2)^6}. \tag{7}$$

Obviously, the output power density is closely related to the size, the number of layers, and the figure-of-merit (FOM) $d_{33} \times g_{33}$ of the crystal wafer.

Compared with the traditional CPEH, the BSPEH has the following three advantages. (i) The structure is more stable, and the piezoelectric elements are less prone to crack as the d_{33} mode is adopted. (ii) The axial stress can be amplified by changing the length of the flange shaft (L_1), as shown in Eq. (1). (iii) The output performance can be multiplied by changing the connection mode of single crystal stacks. For instance, compared to one single crystal stack, two single crystal stacks can get a higher output current in parallel [$I_{p-parallel} = j(2\pi)f(2Q) = 2I_p$] or a higher output voltage in series [$V_{p-series} = \frac{Q}{(nC_0/2)} = 2V_p$], as shown in Eqs. (5) and (6).

B. FEM simulation

The Finite Element Method (FEM) (COMSOL Multiphysics) was employed to verify the output performance and optimize the structure of the energy harvester. The material properties of PIN-PMN-PT single crystals were obtained from the previous work.[17]

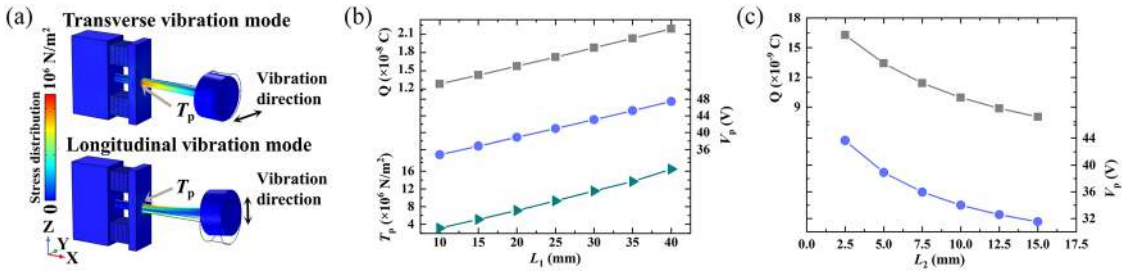

FIG. 2. FEM simulations of the BSPEH. (a) The schematic of vibration modes and the peak stress T_p of the flange shaft. The relationship between the induced charge Q, output open-circuit voltage peak V_p, and L_1 (b) and L_2 (c) in the longitudinal vibration mode.

Figure 2 shows the dependence of the induced charge Q, corresponding output open-circuit voltage peak V_p, and peak stress T_p of the flange shaft on the size of L_1 and L_2 for two single crystal stacks connected in series. The vibration acceleration is 3 g. As shown in Fig. 2(a), we define the symmetric vibration mode along the Z axis as the transverse vibration mode and the symmetric vibration mode along the X axis as the longitudinal vibration mode.

As shown in Fig. 2(b), Q, V_p, and T_p increase with the increase in the flange shaft (L_1), and it coincides with the relationship in Eqs. (4) and (6). In order to make the flange shaft work under the appropriate bending strength, combining T_p [Figs. 2(a) and 2(b)] and the allowable shear stress ([τ], about 40 MPa–60 MPa) of the flange shaft, we set L_1 to be 25 mm. As shown in Fig. 2(c), both Q and V_p decrease with the increase in the distance between two crystal stacks (L_2), and it coincides with the relationship in Eqs. (4) and (6). In this work, considering the diameter of the flange shaft and assembly problems, we set L_2 to be 7.5 mm.

III. RESULTS AND DISCUSSION

A. The performance of BSPEH

Figures 3(a) and 3(b) show the open-circuit voltage of the two crystal stacks as a function of vibration frequency from 250 Hz to 500 Hz at the acceleration of 1 g, 2 g, 3 g, 4 g, and 5 g. The inset of Fig. 3(a) shows the output voltage for transverse and longitudinal vibration modes of the piezoelectric stack by using the FEM simulation, corresponding to ~350 Hz and 390 Hz, respectively. Obviously, at 390 Hz, the output voltage of the stack is the largest, about 24 V_{p-p}. According to the FEM results, the single crystal stacks are in a state of half compression and half tension when the BSPEH is in the transverse vibration mode [Fig. 2(a)], so the output performance of this mode has a subtraction effect. This explains the relatively low output voltage at 350 Hz (transverse vibration mode) compared with 390 Hz (longitudinal vibration mode). In addition, the output voltages of the two stacks are almost the same, indicating that the BSPEH is well assembled and forced uniformly.

Figures 3(c) and 3(d) display the short-circuit current and output power of the two stacks (which are calculated using the effective value of the output voltage) under various load resistances (R_{load}) measured at a frequency of 390 Hz and an acceleration of 5.0 g. In addition, the maximum output current is about 530 μA. With the increase in R_{load}, the maximum output power is about 4.3 mW and the power density is up to 39.7 mW cm^{-3}. As we know, when R_{load} matches the internal resistance (R_{inte} ~ 40 kΩ) of the BSPEH, it can output the maximum power. In this case, the resistance satisfies the following formula:

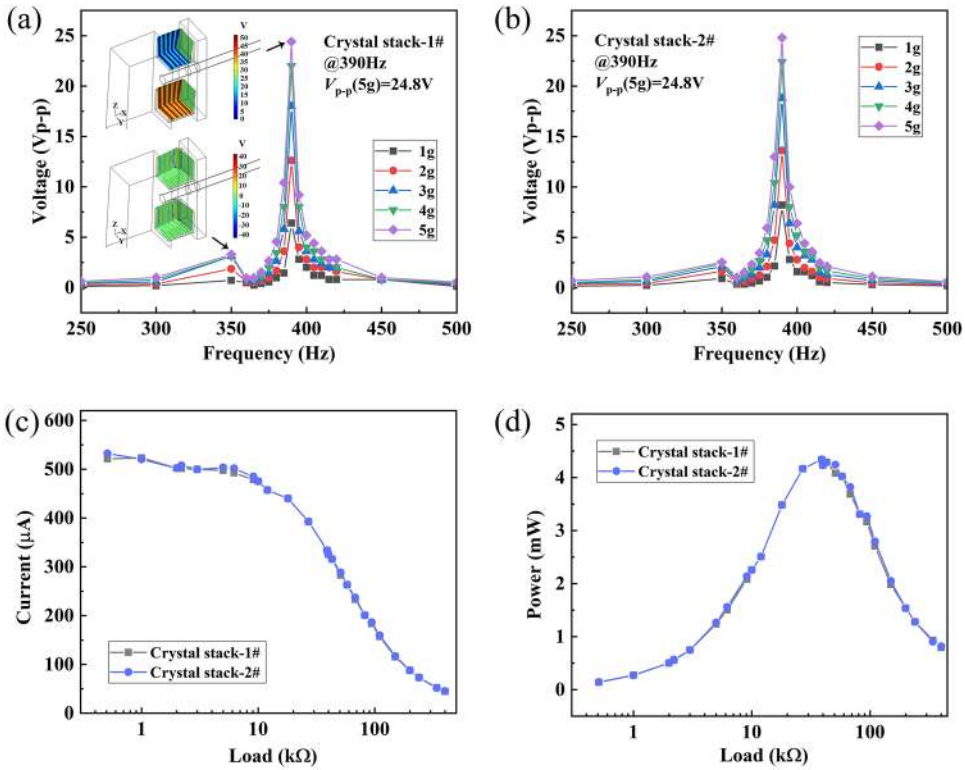

FIG. 3. The performance of the BSPEH energy harvester with one single crystal stack. [(a) and (b)] The output voltages as a function of the frequency for each stack. The inset of (a) shows the output voltage for transverse and longitudinal vibration modes of the BSPEH, and the crystal stacks are connected in series. (c) The output current and (d) the output power as functions of the load resistance (R_{load}) for each stack.

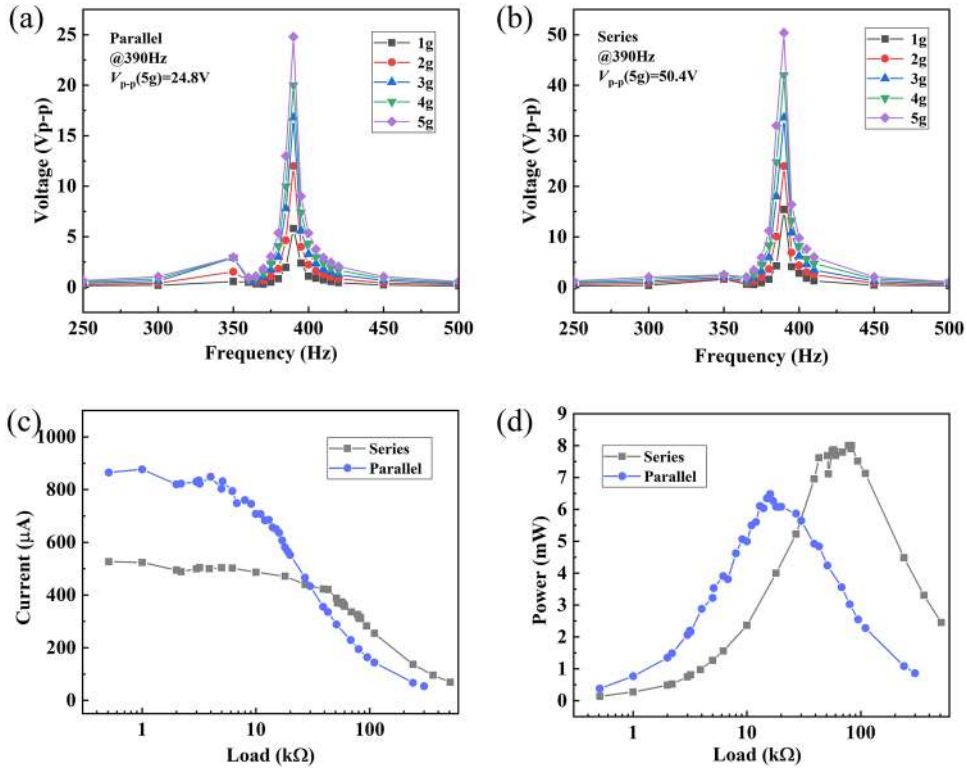

FIG. 4. The performance of the BSPEH connected in parallel and series. The output voltages as a function of the frequency (a) in parallel connection and (b) in series connection. (c) The output current and (d) the output power as functions of the load resistance (R_{load}) in parallel and series connections.

$$R_{load} = R_{inte} = \left| \frac{1}{2j\pi f C_0} \right|. \quad (8)$$

In addition, R_{inte} of BSPEH is almost two orders of magnitude less than a similar ceramic BSPEH.[13]

Figure 4 depicts the output performance of the BSPEH as two crystal stacks are connected in parallel and in series. It can be seen from Figs. 4(a) and 4(b) that different connection modes do not affect the resonant frequency of the device, while V_{p-p} of connecting in series is twice that of parallel because the static capacitance in series is equivalent to half that of parallel. Based on Eq. (5), the output current is proportional to the number of crystal wafers, slightly different from Fig. 4(c), which is caused by the errors and losses in the testing process. As shown in Fig. 4(d), R_{load} (R_{inte}) connected in parallel is about 20 kΩ, which is about 0.25 times of R_{load} (R_{inte}) connected in series. It is consistent with the theoretical value calculated by Eq. (8). This is because the capacitance of two crystal

TABLE I. The BSPEH performance comparison with previous piezoelectric energy harvesters.

Materials	Structures	Maximum output current (μA)	Maximum power density (mW cm^{-3})	References
PNN-PZT-PIN ceramics	Flex-tensional	8	0.1	13
PZT-51 ceramics	Cantilever	...	0.1	19
PZT-4 ceramics	Flex-tensional	...	9.3	9
PMN-PT crystal	Flex-tensional	...	29.3	20
PMN-PT crystal	Cantilever	...	14.8	21
PVDF-TrFE polymer	Bending	1	8.8	22
PVDF-TrFE polymer	Flex-tensional	353	...	4
PIN-PMN-PT crystal	Flex-tensional	600	13.8	5
PIN-PMN-PT crystal	Flex-tensional	880	39.7	This work

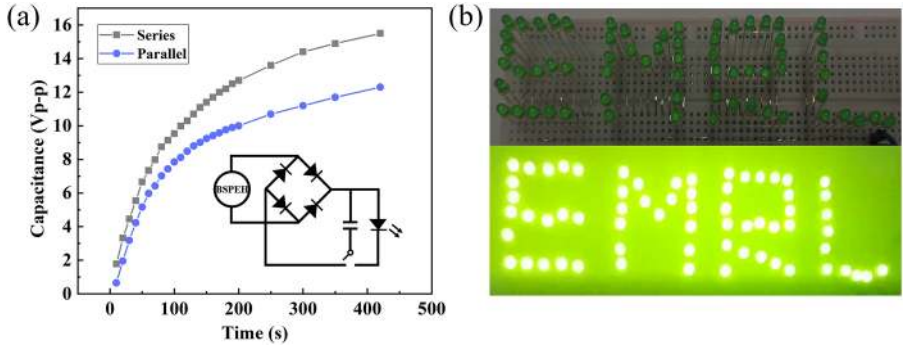

FIG. 5. (a) Charging behavior using the capacitance of 1 mF. The inset shows the equivalent circuit diagram for converting the AC voltage into DC voltage. (b) The LEDs lighted with the capacitance.

stacks connected in parallel is four times that of two crystal stacks connected in series. For the voltage source, lower R_{inte} is equal to the higher energy conversion efficiency. Hence, the parallel connection is preferable because of the lower R_{inte} and the higher output current.[18] Table SI of the supplementary material shows the piezoelectric properties of the PIN-PMN-PT single crystal and piezoelectric ceramics. The $d_{33} \times g_{33}$ value of the PIN-PMN-PT single crystal wafer is more than two times larger than ceramics. Due to the high value of $d_{33} \times g_{33}$ (4.693×10^{-11} C V mN^{-2}), the maximum output power densities of the BSPEH in parallel and series connections are 30.0 mW cm^{-3} and 36.9 mW cm^{-3}, respectively, higher than the advanced energy harvesters made of piezoelectric ceramics, PMN-PT crystals, or new functional polymer materials (as shown in Table I).

B. The application of BSPEH

Figure 5(a) shows the voltage for a capacitor of 1 mF charged by using the BSPEH at an acceleration of 5 g and a frequency of 390 Hz. The inset of Fig. 5(a) shows a full-wave rectifying bridge for converting the AC voltage to the DC output voltage. It can be seen that the saturation time of series and parallel connections was about 400 s, which depends on the internal resistance and saturation voltage.[5] The charged capacitor was then used to drive 65 commercial LEDs (the threshold voltage of 1.8 V) connected in parallel [Fig. 5(b)]. The results indicate that the BSPEH can enable self-powering of wireless sensor networks in a vibrating circumstance.

C. Fatigue characteristics of the energy harvesters

To investigate the stability and durability of the harvester under vibration excitation, we compare the fatigue characteristics of the BSPEH and CPEH at resonance frequencies (f_r) (390 Hz and 52 Hz), respectively [Figs. 6(a) and 6(b)]. The BSPEH and CPEH were measured with the same tip force of ~0.25 N under the vibration acceleration of 5 g and 2 g, respectively. Figure 6(a) shows the fatigue curves, and Fig. 6(b) shows the percentage decline of the output voltage for the BSPEH and CPEH.

During the durability test, the output voltage of BSPEH almost remained constant, while that of CPEH decreased by about 20%. This indicates that under the large vibration excitation and more than 10^6 vibration cycles, the BSPEH exhibits a very stable output performance. Table II shows the performance changes of piezoelectric materials in the energy harvesters before and after testing the cycling stability (applying dynamic pressure at f_r over 10^5 cycles). It can be found that the piezoelectric property of the piezoelectric elements in CPEH reduced in certain degree, while the piezoelectric stacks in BSPEH remained nearly constant. Hence, the degradation of CPEH may be caused by the crack of the ceramic; furthermore,

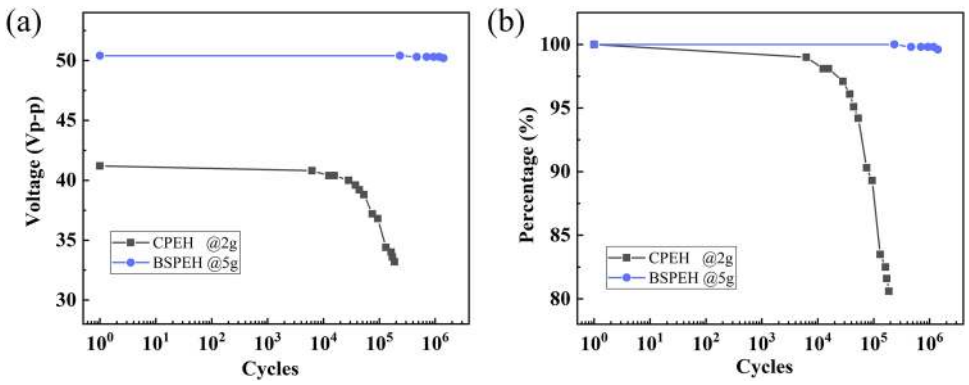

FIG. 6. Fatigue characteristics of the BSPEH and the CPEH. (a) The change of output voltage. (b) The percentage decline of the output voltage.

TABLE II. The performance changes of piezoelectric materials in the energy harvesters before and after the durability test.

Structure	Piezoelectric elements	d_{33} (pC/N)			$\varepsilon_{33}^T/\varepsilon_0$			tan δ (%)		
		Before testing	After testing	Variation (%)	Before testing	After testing	Variation (%)	Before testing	After testing	Variation (%)
BSPEH	PIN-PMN-PT crystal (#1)	10 780	10 770	0.1	320 700	320 500	0.1	1.03	1.12	8.7
	PIN-PMN-PT crystal (#2)	11 220	11 220	0.0	322 900	322 600	0.1	1.11	1.20	8.1
CPEH	PZT-5H ceramic	650	610	6.2	3500	3280	6.3	1.29	1.64	27.1

it may also be caused by the low adhesion between the piezoelectric element and epoxy in the cantilever structure,[12,23] which leads to the failure of the bonding during the vibration. For conventional cantilever structures, one side of the piezoelectric element is connected to the cantilever by epoxy and the other side of the piezoelectric element is in a free state, so it is easy to be loose during the vibration process, resulting in reducing the strain of the piezoelectric element. On the other hand, for BSPEH, the piezoelectric elements are pre-pressed with a bolt, and it is much stronger compared with the CPEH. Thus, the output performance of BSPEH is quite stable compared with the CPEH, as shown in Fig. 6, demonstrating that BSPEH has potential applications in the ambient environment needing long time working and having a large vibration acceleration.

IV. CONCLUSIONS

In summary, we proposed a barbell-shaped piezoelectric energy harvester (BSPEH) based on multilayer PIN-PMN-PT single crystal stacks. The stack consists of ten layers of crystal plates glued in opposite polarity one by one (i.e., in parallel connection) and operated in the d_{33}-mode under vibration excitation. The BSPEH shows the maximum output voltage of 50.4 V_{p-p} with the two crystal stacks connected in series, and the maximum output current of 880 μA with the two crystal stacks connected in parallel, and the maximum output power density of 39.7 mW cm^{-3} under the cyclic force of ~0.25 N. In addition, since the piezoelectric stack is in a clamping state during working, it can withstand a large vibration excitation. The performance of BSPEH was almost not changed after 10^6 vibration cycles at an acceleration of 5 g and a frequency of 390 Hz, showing strong vibration durability compared to traditional cantilever energy harvesters (the performance decreased by 20% after 10^5 cycles). All these features indicate that the newly designed BSPEH has a great application potential to be used in the self-powered devices and wireless sensors with a large vibration environment.

V. EXPERIMENTAL SECTION

A. Fabrication of the energy harvester

In this paper, the [001]-oriented rhombohedral (R) phase PIN-PMN-PT crystal was selected, which was grown by the modified Bridgman technique.[24] The x-ray diffraction pattern of the crystal is shown in Fig. S1 of the supplementary material. According to the phase diagram of the PIN-PMN-PT system,[25] the composition is around 0.33PIN-0.38PMN-0.29PT. Then, the crystal was cut into pieces with a dimension of 5 × 5 × 0.5 mm^3, and the three edges were parallel to [100]/[010]/[001] in the pseudocubic coordinate system. The gold electrode was sputtered on the (001) surface like the "crystal wafer" shown in Fig. 1(b). At room temperature, all wafers were polarized in silicone oil for five minutes under a 10 kV/cm DC electric field (d_{33} ~ 1300 pC/N). Then, with epoxy (Epo-Tek 301), ten crystal plates were glued together in opposite polarity to form a mechanical series and electrical parallel structure. In addition, two pieces of alumina ceramics (5 × 5 × 0.3 mm^3) were used as upper and lower end caps to protect the piezoelectric stacks. Vacuum sputtered gold as the external electrodes was applied to make electrical contact with the alternate edges of the internal electrodes just like the "crystal stack" shown in Fig. 1(b). Follow the above steps to make at least two piezoelectric stacks. In addition, d_{33} of a complete stack is ~11 000 pC/N. Finally, the designed spring steel shell, tip mass, and single crystal stacks were fixed together by nuts to form a complete BSPEH.

The traditional d_{31}-mode unimorph CPEH was fabricated using commercial PZT-5H ceramics (30 × 5 × 0.5 mm^3), and the tip mass was 10 g.

B. Measurement of the energy harvester

The experimental setup is shown in Fig. S2 of the supplementary material. The sinusoidal wave generated by the signal generator (DG1032Z, Rigol Technologies, China) is fixed onto the vibration exciter (HEV-200, Nanjing Foneng Tech Co., China) after passing through the voltage amplifier (HEA-200C, Nanjing Foneng Tech Co., China). Then, the vibration exciter drives the energy harvester and accelerometer (CT1010L, Shanghai Chengtec Electronics Co., China) fixed on the vibration platform. The output voltage of the energy harvester and accelerometer is measured with an oscilloscope (DS1054, Rigol Technologies, China). In this paper, the output electrical properties of a single piezoelectric stack and two piezoelectric stacks in series and parallel are tested, and the full-wave rectifying circuit, as shown in Fig. 5(a), is used to charge the capacitance of 1 mF. 65 parallel LEDs were successfully lit.

SUPPLEMENTARY MATERIAL

See the supplementary material for the details on the piezoelectric properties of the PIN-PMN-PT crystal and piezoelectric ceramics, the x-ray diffraction pattern, and the vibration energy harvesting test setup.

ACKNOWLEDGMENTS

This work was supported by the National Natural Science Foundation of China (Grant Nos. 52002312 and 51922083), the China Postdoctoral Science Foundation (Grant No. 2019M663720), and the Fundamental Research Funds for the Central Universities (Grant Nos. xzy012020005, xxj022019034, and xpt012020025).

DATA AVAILABILITY

The data that support the findings of this study are available from the corresponding author upon reasonable request.

REFERENCES

[1] J. Ryu, J.-E. Kang, Y. Zhou, S.-Y. Choi, W.-H. Yoon, D.-S. Park, J.-J. Choi, B.-D. Hahn, C.-W. Ahn, J.-W. Kim, Y.-D. Kim, S. Priya, S. Y. Lee, S. Jeong, and D.-Y. Jeong, Energy Environ. Sci. **8**, 2402 (2015).
[2] H. E. Lee, J. H. Park, D. Jang, J. H. Shin, T. H. Im, J. H. Lee, S. K. Hong, H. S. Wang, M. S. Kwak, M. Peddigari, C. K. Jeong, Y. Min, C. H. Park, J.-J. Choi, J. Ryu, W.-H. Yoon, D. Kim, K. J. Lee, and G.-T. Hwang, Nano Energy **75**, 104951 (2020).
[3] E. Shagdar, B. G. Lougou, Y. Shuai, J. Anees, C. Damdinsuren, and H. Tan, Appl. Energy **264**, 114744 (2020).
[4] X. Yuan, X. Gao, J. Yang, X. Shen, Z. Li, S. You, Z. Wang, and S. Dong, Energy Environ. Sci. **13**, 152 (2020).
[5] X. Gao, C. Qiu, G. Li, M. Ma, S. Yang, Z. Xu, and F. Li, Appl. Energy **271**, 115193 (2020).
[6] F. R. Fan, W. Tang, and Z. L. Wang, Adv. Mater. **28**, 4283 (2016).
[7] F.-R. Fan, Z.-Q. Tian, and Z. Lin Wang, Nano Energy **1**, 328 (2012).
[8] Y. Zhou, D. J. Apo, and S. Priya, Appl. Phys. Lett. **103**, 192909 (2013).
[9] X. Li, M. Guo, and S. Dong, IEEE Trans. Ultrason. Ferroelectr. Freq. Control **58**(4), 698 (2011).
[10] M. Ma, S. Xia, Z. Li, Z. Xu, and X. Yao, Appl. Phys. Lett. **105**, 043905 (2014).
[11] B. Ren, S. W. Or, X. Zhao, and H. Luo, J. Appl. Phys. **107**, 034501 (2010).
[12] J. Wu, X. Chen, Z. Chu, W. Shi, Y. Yu, and S. Dong, Appl. Phys. Lett. **109**, 173901 (2016).
[13] X. Gao, J. Wu, Y. Yu, and S. Dong, Appl. Phys. Lett. **111**, 212904 (2017).
[14] S. Zhang, F. Li, X. Jiang, J. Kim, J. Luo, and X. Geng, Prog. Mater. Sci. **68**, 1 (2015).
[15] S. Zhang and F. Li, J. Appl. Phys. **111**, 031301 (2012).
[16] Z. Zeng, B. Ren, L. Gai, X. Zhao, H. Luo, and D. Wang, IEEE Trans. Ultrason. Ferroelectr. Freq. Control **63**(8), 1192 (2016).
[17] E. Sun, R. Zhang, F. Wu, and W. Cao, J. Alloys Compd. **553**, 267 (2013).
[18] H. Liu, C. Quan, C. J. Tay, T. Kobayashi, and C. Lee, Phys. Procedia **19**, 129 (2011).
[19] J. Zhao, X. Zheng, L. Zhou, Y. Zhang, J. Sun, W. Dong, S. Deng, and S. Peng, Smart Mater. Struct. **21**, 105006 (2012).
[20] B. Ren, Y. Zhang, Q. Zhang, X. Li, W. Di, X. Zhao, H. Luo, and S. W. Or, Appl. Phys. A **100**, 125 (2010).
[21] C. Xu, B. Ren, W. Di, Z. Liang, J. Jiao, L. Li, L. Li, X. Zhao, H. Luo, and D. Wang, Appl. Phys. Lett. **101**, 033502 (2012).
[22] L. Zhang, J. Gui, Z. Wu, R. Li, Y. Wang, Z. Gong, X. Zhao, C. Sun, and S. Guo, Nano Energy **65**, 103924 (2019).
[23] D. K. Bharti, M. K. Gupta, R. Kumar, N. Sathish, and A. K. Srivastava, Nano Energy **73**, 104821 (2020).
[24] X. Wang, Z. Xu, Z. Li, F. Li, H. Chen, and S. Fan, Ferroelectrics **401**, 173 (2010).
[25] J. Chen, X. Li, X. Zhao, X. Wang, C. Chen, H. Deng, B. Ren, J. Jiao, and H. Luo, J. Mater. Sci.: Mater. Electron. **26**, 9316 (2015).